Near-surface velocity estimation by weighted early-arrival waveform inversion

Xukai Shen

ABSTRACT

In this paper, I present a modified version of the conventional waveform inversion objective function to bridge the gap between the acoustic waveform inversion engine and the more complicated physics in recorded data. The proposed method weighs the amplitude of observed and modeled data. In this way, I use more of the phase information rather than the amplitude information in recorded data. Since phase information is more robust in the presence of visco-acoustic or even elastic related physics. Synthetic examples with inversion of visco-acoustic data and elastic data show that using the proposed objective function can recover detailed velocity structures even with the presence of non-acoustic physics, while conventional waveform inversion tends to fail.

INTRODUCTION

Near-surface velocity is important for imaging deeper targets. Complex near-surface velocity can cause serious problems for imaging deeper targets if it is not accurately estimated. Conventionally, people use ray-based methods (Hampson and Russell, 1984; Olson, 1984; White, 1989) to derive the large-scale structure of near-surface velocity. Such smooth velocity structure may be adequate for areas with simple near-surface velocity. However, in geologically complex areas, smooth velocity is not accurate enough for imaging deeper reflectors (Marsden, 1993; Bevc, 1995; Hindriks and Verschuur, 2001). In such cases, waveform inversion (Tarantola, 1984; Pratt et al., 1998; Mora, 1987) tends to give more accurate results (Ravaut et al., 2004; Sheng et al., 2006; Sirgue et al., 2009) by using finite-frequency seismic wave propagation.

Yet there are several important factors for practical application of waveform inversion. Among these are the quality of the starting velocity model, the accuracy of the source wavelet estimation, and the complexity of physics in the recorded data and the inversion engine. In addition to the P-wave velocity, the density, S-wave velocity, anisotropy parameters, attenuation and other factors all affect the recorded data. When compared with data modeled from the constant-density acoustic wave equation, these extra parameters will not only change the amplitude and phase of existing events, but they also may add extra events, such as converted waves. However, there are several problems associated with inverting these parameters. First, they are much less well constrained than the P-wave velocity, so it is much more difficult to

invert all these parameters than just P-wave velocity. Second, it is more computationally expensive to incorporate all these parameters into the wave-equation engine used in inversion; for example, modeling using the elastic wave equation is at least an order of magnitude more expensive than using the acoustic wave equation. Thus the acoustic wave equation is still the most practical waveform inversion engine so far. With this choice, however, the objective function of conventional waveform inversion is inadequate to bridge the gap between the physics of the data and the physics of the inversion engine.

It is known that traveltime/phase information is less sensitive to the presence of different physics in the recorded data and also carries the information about velocity field (Luo and Schuster, 1990; Shin and Min, 2006). In conventional waveform inversion, both phase and amplitude information of the modeled data are compared with recorded data. I modify the objective function of waveform inversion, giving added weight to the match of phase information in the modeled and the recorded data for each iteration of the inversion. I do not match the recorded and modeled data by subtracting their phases, thus avoiding the ambiguity caused by phase wrapping (Shin and Min, 2006).

THEORY

The generalized waveform inversion objective function can be written as

$$f\left(\mathbf{d_{obs}}, \mathbf{D(m)}\right) \approx \mathbf{0}, \tag{1}$$

where f is a function of $\mathbf{d_{obs}}$, observed data and $\mathbf{D(m)}$, forward modeled synthetic data from $\mathbf{m}$, the velocity model. Observed data can be in either the frequency domain or the time domain, depending on the actual form of $\mathbf{f}$. For example if we take $\mathbf{f}$ as the L2 norm of $(\mathbf{d_{obs}} - \mathbf{D(m)})$, we obtain the objective function of conventional waveform inversion (Tarantola, 1984; Pratt et al., 1998); if we take $\mathbf{f}$ as the L2 norm of natural logarithm of $\mathbf{D(m)}/\mathbf{d_{obs}}$, we obtain the so called logarithmic objective function of waveform inversion (Shin and Min, 2006). However, direct comparison in the phase domain will encounter the problem of phase wrapping. I modify the objective function of conventional waveform inversion by using the following expression for $\mathbf{f}$:

$$\begin{aligned} f &= \sum_{\mathbf{s},\mathbf{r}} \|\delta \mathbf{d}(\mathbf{s},\mathbf{r})\|^{\mathbf{2}} \\ &= \| \frac{\mathbf{D}(\mathbf{s},\mathbf{r},\mathbf{m})}{\sqrt{\mathbf{D^T}(\mathbf{s},\mathbf{r},\mathbf{m})\mathbf{D}(\mathbf{s},\mathbf{r},\mathbf{m})}} - \frac{\mathbf{d_{obs}}(\mathbf{s},\mathbf{r})}{\sqrt{\mathbf{d_{obs}^T}(\mathbf{s},\mathbf{r})\mathbf{d_{obs}}(\mathbf{s},\mathbf{r})}} \|^{\mathbf{2}} \end{aligned} \tag{2}$$

where $\mathbf{m}$ is the model, which consists of near-surface velocity; $\mathbf{d_{obs}}$ are the data, which consist of band-passed early arrivals of the wavefield. Data are filtered based on traveltime difference before bandpassing to exclude events that come relatively late in the early arrivals. $\mathbf{D}$ is the constant-density two-way acoustic wave-equation

operator that generates synthetic early arrivals from source and near-surface velocity; **s** and **r** are source and receiver locations, respectively. In the new objective function, I weight both recorded data and forward-modeled data by their RMS energy trace by trace. This ensures that the recorded data and the forward-modeled data have relatively the same amplitudes, and waveform inversion in this case will focus more on phase comparison. To update the velocity, I use the nonlinear conjugate gradient method. The gradient of equation 2 with respect to **m** is as follows:

$$\mathbf{J_F(m)} = \mathbf{2}\delta\mathbf{d^T(s,r)}\frac{\partial\left(\frac{\mathbf{D(s,r,m)}}{\sqrt{\mathbf{D^T(s,r,m)D(s,r,m)}}}\right)}{\partial\mathbf{m}} \tag{3}$$

After some algebraic manipulations, equation 2 becomes:

$$\mathbf{J_f(m)} = \mathbf{2V_{src}}\frac{\partial\mathbf{D(s,r,m)}}{\partial\mathbf{m}} \tag{4}$$

where $\mathbf{V_{src}}$ is defined as

$$\begin{aligned}\mathbf{V_{src}} &= \frac{\delta\mathbf{d(s,r)}}{\sqrt{\mathbf{D(s,r,m)^T D(s,r,m)}}} \\ &+ \frac{\delta\mathbf{d^T(s,r)D(s,r,m)}}{\mathbf{D(s,r,m)^T D(s,r,m)}}\mathbf{D(s,r,m)}\end{aligned} \tag{5}$$

For gradient calculation, the only difference between conventional waveform inversion and weighted waveform inversion is how to calculate the virtual source. In conventional waveform inversion, the difference between observed data and modeled data is used as virtual source for reverse-time propagation. In weighted waveform inversion, a new virtual source defined in 5 is used for reverse-time propagation.

The step length calculation assumes local parabolic behavior of the objective function (Vigh and Starr, 2008). I first obtain two different perturbations of the velocity $\delta\mathbf{m}$ by scaling the gradient to about three percent of the minimum value in the current velocity; then I calculate the misfit function value, and determine the minimum of the parabola by using the two perturbation step length $\alpha_\mathbf{1}$ and $\alpha_\mathbf{2}$ and the existing velocity $\alpha_\mathbf{0} = \mathbf{0}$.

In the synthetic example shown next, I assume a known source wavelet in both examples. I carry out the waveform inversion using several frequency bands, starting from low frequency and gradually moving to higher frequency (Sirgue and Pratt, 2004). The inversion result of each frequency range is used as the starting model for inversion in the next frequency range. Using the low-frequency component of the data ensures good estimation of long-wavelength components of the velocity model, and subsequent higher-frequency inversion will retrieve finer velocity structures. As will be shown later, inversion results using this objective function are robust when we have attenuation or elastic waves in the recorded data.

EXAMPLES

To illustrate the idea, I show two examples of acoustic inversion of data generated with wave equations contain more complex physics than pure acoustics. The first example uses data generated by the visco-acoustic wave equation, which means there is attenuation in the subsurface that causes phase/amplitude change in the data. The second example uses data generated by the elastic wave equation. This not only changes the phase/amplitude of existing events relative to data generated by acoustic wave equation, but also add extra events which are converted modes. However in both cases, by carefully masking out non-acoustic events and focusing on the phase of "acoustic-equivalent" data, acoustic inversion can still produce a good estimate of near-surface velocity.

Data recorded with strong subsurface attenuation

Here I estimate near-surface velocity using recorded data with strong subsurface attenuation. The model is from Amoco-2.5D synthetic velocity model. The Q value is a scaled version of velocity to maintain consistency between structures. The velocity model is 600 by 140 grid in x and z, with 10 m spacing in both directions. The acquisition geometry is relatively simple. Receivers are on all the grid points on the surface, there are 30 shots with uniform spacing of 100 m.

A shot gather at a single location from data is shown in figure 1; the left panel shows the data without attenuation, and the right panel shows the data with attenuation. It can be seen that the attenuated data has lower frequency content and much weaker amplitude. However, the kinematics of the data does not change much. Thus, in this case, phase information in the data is relatively insensitive to non-acoustic physics in the recorded data. Figure 2 shows the true near-surface velocity and starting velocity model. The results of estimated velocity using conventional waveform inversion fitting goals and weighted waveform inversion fitting goal are shown in figure 3. It can be seen that with strongly attenuated data, weighted waveform inversion is still able to recover the velocity model, while conventional fitting goal completely fails in this case. Since conventional waveform inversion use both phase and amplitude information in the recorded data, it tries to interpret weak amplitude as a result of a fast velocity layer at the surface. The new objective function, however, focuses more on phase information and partially ignores amplitude information to give a much better result.

Data recorded with elastic wave equation

Next I estimate the the near-surface velocity using recorded data that is generated by the elastic wave equation. The synthetic P-wave velocity model used in this case is provided by Saudi Aramco. It simulates typical near-surface velocity encountered in

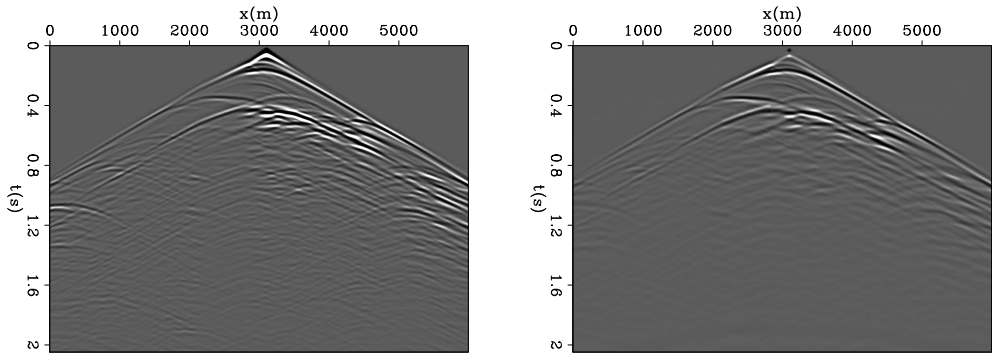

(a) (b)

Figure 1: One synthetic shot with and without attenuation. Both panels have the same clip value. a) One shot generated by the acoustic wave equation. b) Same shot gather generated by the visco-acoustic wave equation with the amplitude of the entire shot gather scaled by a factor of ten.

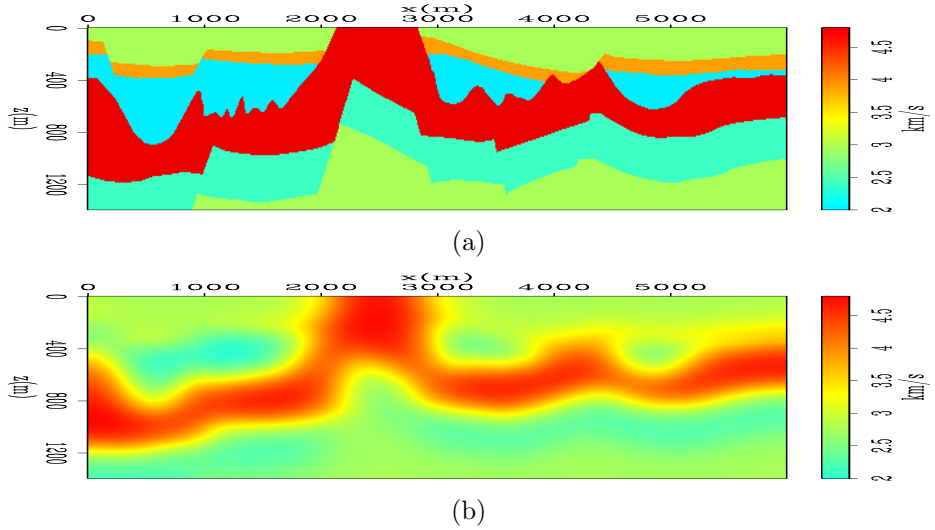

(a)

(b)

Figure 2: a) True near-surface velocity. b) Starting near-surface velocity model used for waveform inversion.

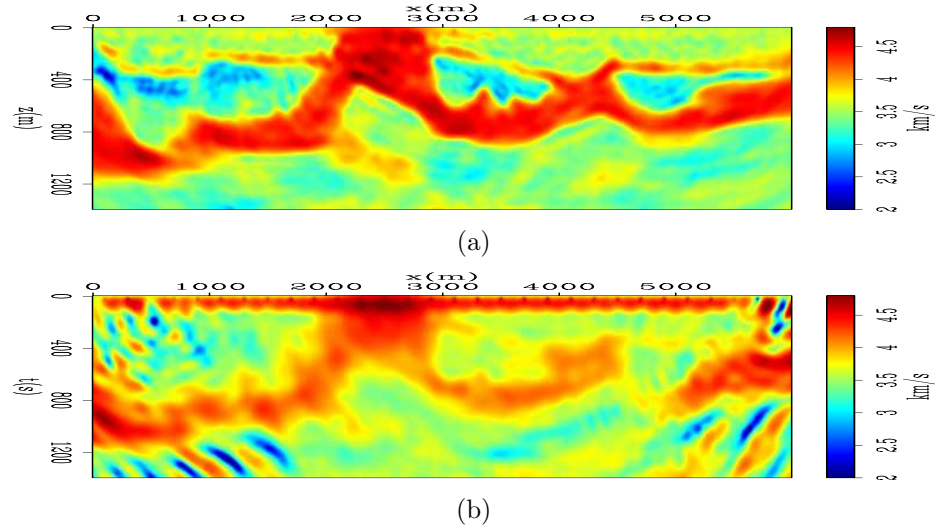

Figure 3: Estimated velocity using different objective functions. a) Estimated velocity using the new objective function. b) Estimated velocity using the conventional objective function.

Saudi Arabia. For elastic modeling, the density is obtained by the Gardner equation (Gardner et al., 1974). S-wave velocity is scaled from P-wave velocity. The model is 1600 by 176 grid in x and z, with 5 m spacing in both directions. The acquisition geometry is also relatively simple. Receivers are on all the grid points on the surface, and there are 90 shots with equal spacing of 80 m. Inversion is done on a 10 m spacing grid, which is coarser than the grid used for modeling. The major goal of acoustic inversion in this case is to see if waveform inversion can retrieve the velocity inversion layer.

One shot gather from data with acoustic and elastic modeling is shown in figure 4; the left panel is the data with acoustic modeling, and the right panel is the data with elastic modeling. It can be seen that data from elastic modeling has some amplitude/phase difference and also some extra events that are converted waves. In this case, I scaled the amplitude of both shots to approximately the same level for display purposes. Figure 5 shows refraction events for the same shot. When I carefully mask out most of the converted waves, the remaining refraction events looks very similar in terms of kinematics; the difference at this point is likely to be caused by different distribution of P-wave and S-wave energy at different reflector boundaries. Figure 6 shows the true near-surface velocity and the starting velocity model; the starting velocity model is a smoothed version of true velocity model. The result of estimated velocity using proposed waveform inversion fitting goal are shown in figure 7. The top panel is the result of inverting acoustic data, whereas the bottom is the result of inverting elastic data. It can be seen that even with strong elastic effects in data, after excluding most converted waves, the weighted fitting goal was still able to recover the velocity inversion structure. Compared with inversion of acoustic data, there are some small shifts of reflector locations. This kind of shift is likely due to

the very sharp velocity contrast immediately below the slow velocity.

This example shows that without the presence of most converted wave, acoustic inversion of elastic data can still obtain a decent velocity estimation result.

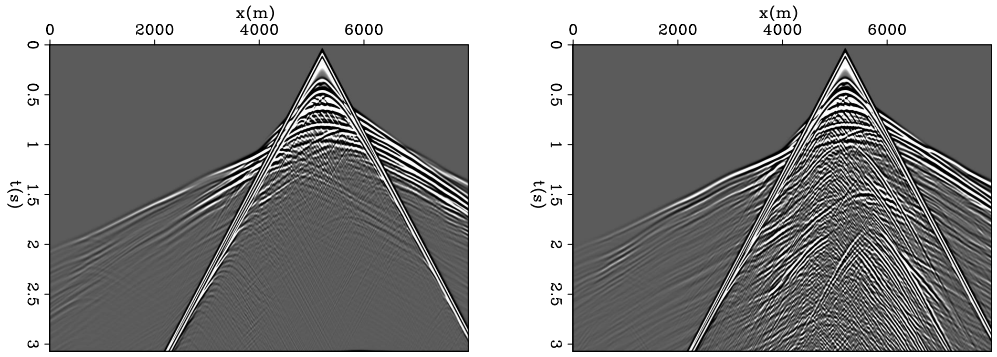

Figure 4: Shot gather generated by different modeling equations: a) shot generated by the acoustic wave equation b) the same shot generated by the elastic wave equation.

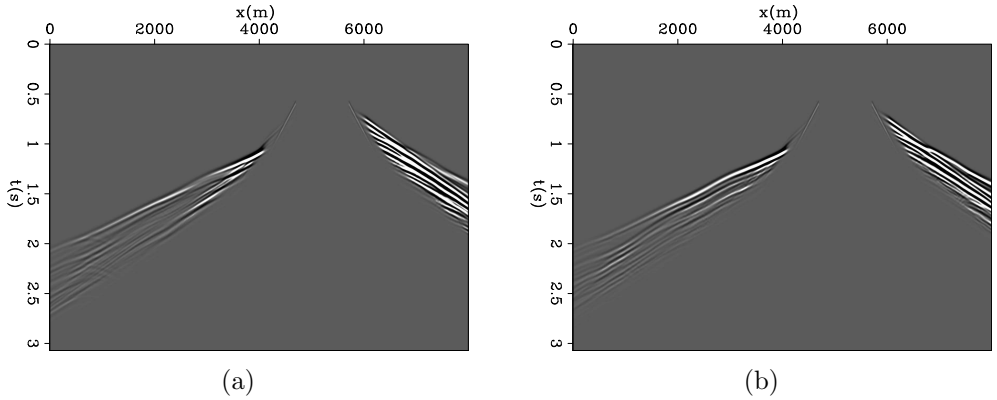

Figure 5: Refraction of the same shot generated by different modeling equations: a) refraction of shot generated by the acoustic wave equation b) refraction of same shot generated by the elastic wave equation.

CONCLUSIONS

The conventional waveform inversion objective function is insufficient when the acoustic wave equation is used in inversion. The insufficiency mainly comes from the fact that non-acoustic physics tend to alter the amplitude and phase of existing events and add new events compared with acoustic data. A new weighted waveform inversion objective function is quite robust, despite the presence of non-acoustic physics in recorded data, and it can recover important velocity structure that can not be detected by conventional ray-based tomography. For the purpose of near-surface velocity estimation, phase information is much less sensitive than amplitude information

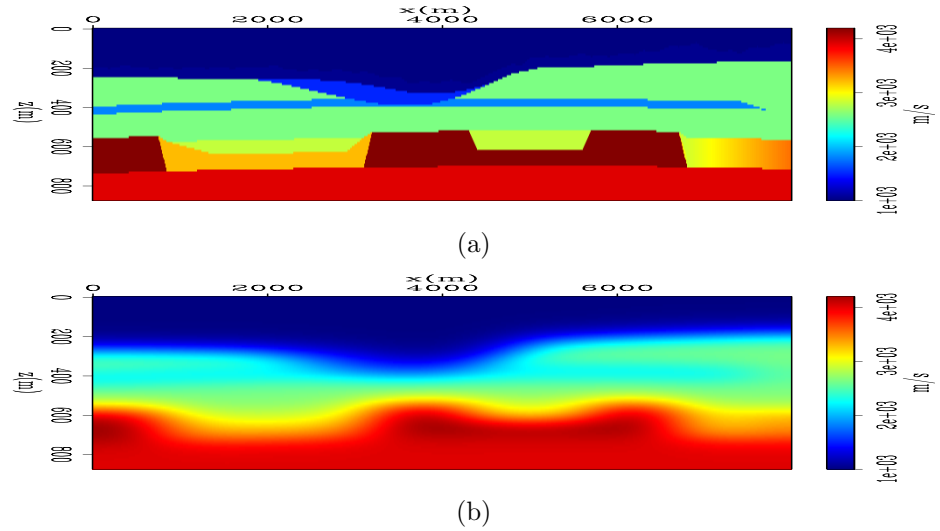

(a)

(b)

Figure 6: a) True near-surface velocity. b) Starting near-surface velocity model used for waveform inversion; the starting velocity model is a smoothed version of the true velocity model.

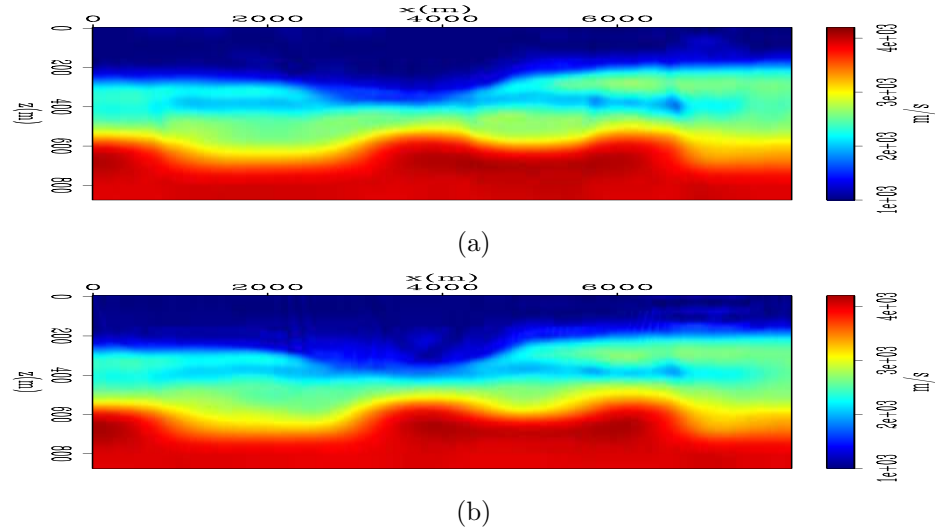

(a)

(b)

Figure 7: Estimated velocity using data from different modeling equations: a) estimated velocity using data generated by the acoustic wave equation. b) Estimated velocity using data generated by the elastic wave equation.

to the presence of non-acoustic parameters, and extra events caused by non-acoustic physics are usually late arriving and can be masked out during waveform matching. The velocity estimation results from this objective function are more stable than conventional waveform inversion.

ACKNOWLEDGMENTS

I would like to thank Stanford Exploration Project for the financial support of this research. Also I would like to thank Saudi Aramco for allowing me to use the synthetic velocity model.

REFERENCES

Bevc, D., 1995, Imaging under rugged topography and complex velocity structure: SEP Ph.D Thesis.

Gardner, G. H. F., L. W. Gardner, and A. R. Gregory, 1974, Formation velocity and density-the diagnostic basics for stratigraphic traps: Geophysics, **39**, 770–780.

Hampson, D. and B. Russell, 1984, First-break interpretation using generalized linear inversion: Journal of CSEG, **20**, 40–54.

Hindriks, C. and D. Verschuur, 2001, Common focus point approach to complex near surface effects: SEG Expanded Abstracts.

Luo, Y. and G. T. Schuster, 1990, Wave-equation traveltime inversion: SEG Expanded Abstracts.

Marsden, D., 1993, Statics corrections-a review: The Leading Edge.

Mora, P., 1987, Elastic wavefield inversion: SEP Ph.D Thesis.

Olson, K. B., 1984, A stable and flexible procedure for the inverse modelling of seismic first arrivals: Geophysical Prospecting, **37**, 455–465.

Pratt, R. G., C. Shin, and G. Hicks, 1998, Gauss-Newton and full Newton methods in frequency domain seismic waveform inversion: Geophysical Journal International, **133**, 341–362.

Ravaut, C., S. Operto, L. Improta, J. Virieux, A. Herrero, and P. Dell'Aversana, 2004, Multiscale imaging of complex structures from multifold wide-aperture seismic data by frequency-domain full-waveform tomography: application to a thrust belt: Geophysical Journal International, **159**, 1032–1056.

Sheng, J., A. Leeds, M. Buddensiek, and G. T. Schuster, 2006, Early arrival waveform tomography on near-surface refraction data: Geophysics, **71**, U47–U57.

Shin, C. and D. J. Min, 2006, Waveform inversion using a logarithmic wavefield: Geophysics, **71**, R31–R42.

Sirgue, L., O.I.Barkved, J. V. Gestel, O. Askim, and R. Kommedal, 2009, 3d waveform inversion on valhall wide-azimuth obc: EAGE 71th Conference.

Sirgue, L. and R. G. Pratt, 2004, Efficient waveform inversion and imaging: A strategy for selecting temporal frquencies: Geophysics, **69**, 231–248.

Tarantola, A., 1984, Inversion of seismic reflection data in the acoustic approximation: Geophysics, **49**, 1259–1266.

Vigh, D. and E. W. Starr, 2008, 3d prestack plane-wave, full-waveform inversion: Geophysics, **73**, 135–144.

White, D. J., 1989, Two-dimensional seismic refraction tomogaphy: Geophysical Journal International, **97**, 223–245.

Biondo L. Biondi graduated from Politecnico di Milano in 1984 and received an M.S. (1988) and a Ph.D. (1990) in geophysics from Stanford. SEG Outstanding Paper award 1994. During 1987, he worked as a Research Geophysicist for TOTAL, Compagnie Francaise des Petroles in Paris. After his Ph.D. at Stanford, Biondo worked for three years with Thinking Machines Co. on the applications of massively parallel computers to seismic processing. After leaving Thinking Machines, Biondo started 3DGeo Development, a software and service company devoted to high-end seismic imaging. Biondo is now Associate Professor (Research) of Geophysics and leads SEP efforts in 3-D imaging. He is a member of SEG and EAGE.

Jon F. Claerbout (M.I.T., B.S. physics, 1960; M.S. 1963; Ph.D. geophysics, 1967), professor at Stanford University, 1967. Emeritus 2008. Best Presentation Award from the Society of Exploration Geophysicists (SEG) for his paper, *Extrapolation of Wave Fields.* Honorary member and SEG Fessenden Award "in recognition of his outstanding and original pioneering work in seismic wave analysis." Founded the Stanford Exploration Project (SEP) in 1973. Elected Fellow of the American Geophysical Union. Authored three published books and five internet books. Elected to the National Academy of Engineering. Maurice Ewing Medal, SEG's highest award. Honorary Member of the European Assn. of Geoscientists & Engineers (EAGE). EAGE's highest recognition, the Erasmus Award.